Fermi surface properties of low-concentration $Ce_xLa_{1-x}B_6$: de Haas–van Alphen

A. A. Teklu,[1] R. G. Goodrich,[1] N. Harrison,[2] D. Hall,[3] Z. Fisk,[3] and D. Young[3]
[1]*Department of Physics and Astronomy, Louisiana State University, Baton Rouge, Lousiana 70803*
[2]*National High Magnetic Field Laboratory, LANL, MS-E536, Los Alamos, New Mexico 87545*
[3]*National High Magnetic Field Laboratory, Florida State University, Tallahassee, Florida 32310*
(Received 7 April 2000; revised manuscript received 17 July 2000)

The de Haas–van Alphen (dHvA) effect is used to study angular-dependent extremal areas of the Fermi surfaces and effective masses of $Ce_xLa_{1-x}B_6$ alloys for x between 0 and 0.05. The dHvA signals from these alloys are observed to change from that arising from the normal two-spin metal, LaB_6, to a single-spin sheet signal at $x=0.05$.

I. INTRODUCTION

The rare earth (RE) and divalent hexaborides have a variety of electrical, magnetic, and thermodynamic properties and all have the same cubic structure. Among these materials are metallic LaB_6,[1] Kondo insulating SmB_6,[2] semimetallic CaB_6,[3–5] heavy-fermion (HF) CeB_6,[6] and ferromagnetic EuB_6.[7] Extensive experimental and theoretical investigations have been done in order to understand their varying physical properties. One of the most decisive techniques to study the electronic properties of these materials is the de Haas–van Alphen (dHvA) effect with which the extremal cross-sectional areas of the Fermi surface (FS) and effective masses can be measured accurately. Pure LaB_6 and pure CeB_6 have been studied using this technique, having nearly identical prolate ellipsoidal FS's, with the FS of CeB_6 being larger than that of LaB_6 by about 10%.[8,9] For example, the values of the dHvA frequencies for LaB_6 and CeB_6 for the same minimum FS ellipsoid cross section are 7.89 and 8.66 kT, respectively. Yet, the effective masses are quite different, being $0.65m_e$ and $30m_e$ (at 5–7 T) for LaB_6 and CeB_6 respectively,[8,9] where m_e is the free-electron mass.

There have been several electrical, magnetic, and thermal studies carried out to explore how this transition from light metallic LaB_6 to the HF CeB_6 takes place when La ions are gradually replaced by Ce ions that introduce $4f$ electrons into the metal. In addition to this, experimental work has been carried out, using the dHvA effect at high magnetic fields (>20 T), to explore the development of the HF behavior in $Ce_xLa_{1-x}B_6$.[10] Here, it was reported that both the FS topology and effective masses transform continuously from that of pure LaB_6 to that of pure CeB_6 as the Ce concentration x is increased from 0 to 1. Furthermore, beginning at very low values of x (about 0.05), the contribution to the dHvA signal was observed to originate from only a single-spin FS sheet.

Here we report detailed dHvA measurements, using both the field modulation technique at intermediate fields (6–15 T) and cantilever torque measurements to 30 T to investigate how the spin polarization manifests itself in the topological changes of the FS, and changes in effective masses of $Ce_xLa_{1-x}B_6$ alloys for $0 \leqslant x \leqslant 0.05$. The results of these measurements are then compared with the previous pulsed field measurements[10] and found to be in excellent agreement. In this paper, the spin dependences of the dHvA signals are investigated both qualitatively and quantitatively, and it is found that the spin-up component dominates the dHvA signal as the Ce concentration increases.

II. EXPERIMENT AND SAMPLE PREPARATION

Single crystals of $Ce_xLa_{1-x}B_6$ with $x=0$, 0.01, 0.02, 0.03, 0.04, and 0.05 were grown in Al flux in the shape of rectangular parallelepipeds ($1\times0.5\times2$ mm) with each face along a [100] axis of the cubic structure. Most of the dHvA magnetization measurements on these samples were made in an NMR calibrated 0–18 T superconducting magnet using the field modulation technique. To verify the reproducibility of the field modulation results, torque measurements on an $x=0.01$ Ce sample were made to 30 T at the National High Magnetic Field Laboratory, Tallahassee, FL.

Using field modulation, constant-angle dHvA measurements were made in the field range 6–15 T with the field direction rotated within a (100) plane. From these fixed-angle–variable-field measurements, one can determine the extremal cross-sectional areas and effective masses from the temperature dependence of signal amplitudes over the entire FS. The sample was further rotated continuously in a fixed field of 10 T to observe the detailed dependences of the FS cross-sectional areas on angle. The above measurements were made at five or six different temperatures in the temperature range of 1.4 K to 4.2 K with the sample immersed in a pumped ^{4}He bath. The sample temperature was measured using a calibrated Cernox thermometer and the vapor pressure of the bath.

III. EXPERIMENTAL RESULTS

Figure 1 shows typical dHvA oscillations for $Ce_xLa_{1-x}B_6$ ($x=0.01$) for $\theta=0°$ (i.e., the applied field in the [100] direction) in the field range of 10–11 T and at a temperature of 1.4 K. A discrete Fourier transform (DFT) of the signal is shown on the same graph. For measurements on pure LaB_6, the frequency of the minimum area or α_3 orbit is found to be 7.894 ± 0.004 kT, which is in good agreement with the original measurements of Arko *et al.*[1] With this as a point of reference, complete angular-dependent studies of the fre-

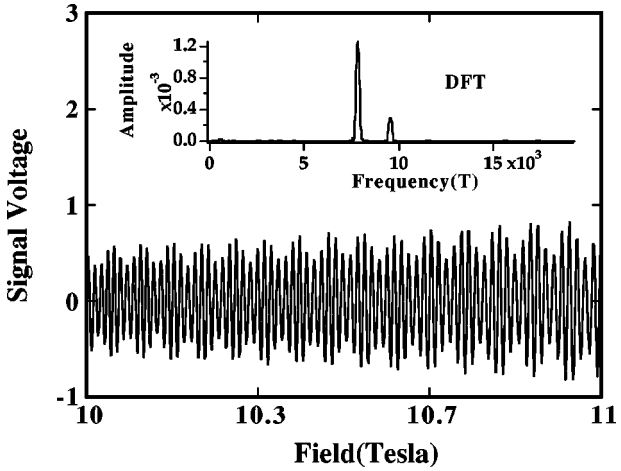

FIG. 1. An example of dHvA oscillations from the field modulation measurements for $x = 0.01$ sample for H along the [100] axis. The inset shows the DFT of the oscillations for a field range of 10–11 T.

quencies in all of the Ce concentrations were made. This study was made in order to check the assumption that the FS is represented by an ellipsoid of revolution, because this assumption had previously been used to calculate FS volumes.[10] Both constant-angle field sweeps and constant-field angle sweeps were obtained. Example data from the constant field rotation measurements for $x=0.01$ at $T=1.4$ K and $H=10$ T is shown in the inset of Fig. 2. The oscillations with angle are caused by the fact that the dHvA phase, $2\pi F(\theta)/H$, changes by 2π for each complete oscillation as θ is varied. The angular variation of F can be determined from these rotation measurements using the counting method first implemented by Halse.[12] Using this technique, the angular variations of the minimum area or α_3 and maximum area or $\alpha_{1,2}$ orbits were obtained. As a further check, field-dependent measurements and DFT's were also made at several angles. An example of the complete data for $x = 0.01$ is shown in Fig. 2.

The effective masses of the different samples ($0 \leqslant x$

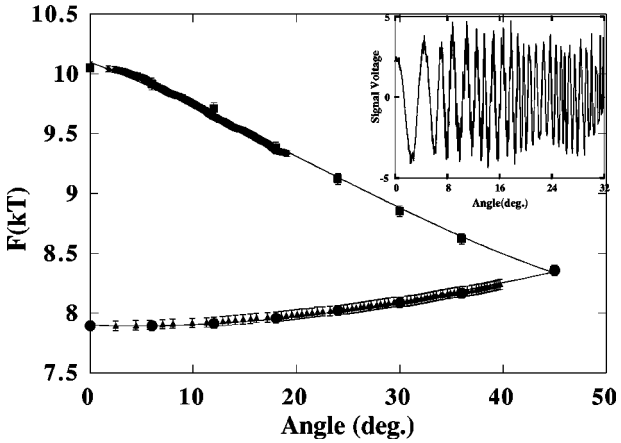

FIG. 2. The dHvA frequencies F_3 and $F_{1,2}$ as a function of orientation for $x=0.01$ from field sweep and rotation (high density points in the figure) measurements. The solid lines are the fits to the to the ellipsoid, Eq. (1). The inset shows the raw data from angular sweep measurements at 10 T.

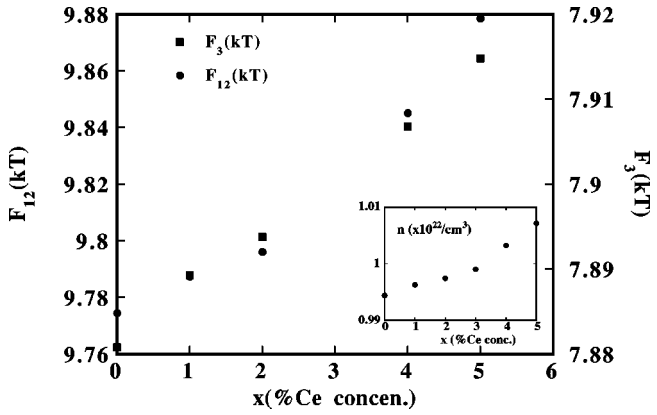

FIG. 3. Ce concentration dependence of the dHvA frequencies F_3 and $F_{1,2}$ at fields 10–11 T. The inset shows the number of electrons per unit volume, n, as a function of x.

$\leqslant 0.05$) are extracted from the temperature dependences of the oscillation amplitudes. In comparison, the value of the effective mass of the α_3 orbit for $x=0$ or pure LaB_6 was found to be $(0.66 \pm 0.03)m_e$ compared to the results of Arko *et al.*,[1] which give $0.65m_e$. Thus, the two values are the same to within experimental uncertainty.

IV. DISCUSSION

From the measured values of the dHvA frequencies, the extremal cross-sectional areas of the α_3 and $\alpha_{1,2}$ orbits for the field applied along the [100] crystal axis of Ce concentrations between $x=0$ and $x=0.05$ can be calculated. As shown in Fig. 3, both of the frequencies corresponding to the α_3 and $\alpha_{1,2}$ orbits are observed to increase with x. From these two frequencies, the volume of the FS, and hence the number of charge carriers per unit volume can be evaluated assuming that the FS is an ellipsoid of revolution.[11] The x dependence of the carrier density n calculated in this manner is shown in the inset of Fig. 3.

It has been reported that both LaB_6 and CeB_6 have similar prolate electron ellipsoidal FS's situated at the six X points of the cubic Brillouin zone (BZ) that overlap along the ΓR symmetry axes.[10,13] This situation is shown schematically in Fig. 4. The minimum cross-sectional area of the ellipse corresponding to the α_3 orbit can be measured directly by applying the magnetic field **H** along the [100] axis, while the maximum area for the $\alpha_{1,2}$ orbit is only observed through magnetic breakdown (MB) for this same field orientation.[10] MB through the necks also leads to a multitude of frequencies $\alpha_{1,2}+n\rho$ within the ΓXM plane, ρ being the frequency of the orbit associated with a small FS orbit inside the necks and n an integer.[14] The value of ρ is $\sim 4-8$ T,[15] which is smaller than our experimental uncertainty, and therefore cannot be resolved at the fields used for our measurements.

The expected angular dependence of the dHvA frequency from an ellipsoid of revolution is[16]

$$\frac{1}{F(\theta)} = A\cos^2\theta + B\sin^2\theta + C\sin\theta\cos\theta. \qquad (1)$$

Here $F(\theta)$ is the dHvA frequency and θ is the angle of

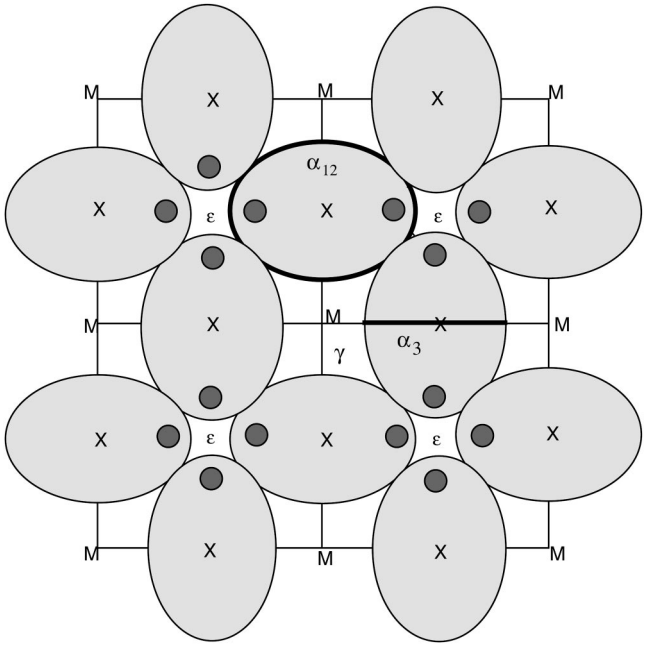

FIG. 4. FS of LaB_6.

rotation from the principal axis of the ellipsoid normal to the field direction. A fit of the data to this equation is a useful criterion for deciding whether or not the FS is an ellipsoid of revolution.[16] We are interested here in the angular variations of the α_3 and $\alpha_{1,2}$ orbits. If the [100] axis is rotated through an angle relative to the field direction in the (100) plane, the cross-sectional area of the FS normal to the field direction corresponding to the semiminor axis of the ellipse, or the α_3 orbit, increases while the one corresponding to the semimajor axis or the $\alpha_{1,2}$ orbit decreases, and these two areas or frequencies become degenerate at 45° (see Fig. 2). These two frequencies and their fit to Eq. (1) are plotted on the same graph in Fig. 2, showing excellent agreement between the expected angular dependence from ellipsoidal FS and the data. This same agreement is obtained for all of the samples with $0 \leqslant x \leqslant 0.05$ measured here. Thus, all of the measurements support the assumption used previously[9,10] that the FS is an ellipsoid of revolution.

Figure 5 shows the concentration (x) dependence of m* for the α_3 orbit, and the fit to the data has the quadratic form: $m^* = m_e(c + bx + ax^2)$. According to Gor'kov and Kim, a linear dependence of the specific heat coefficient γ (proportional to m^*) and the magnetic susceptibility χ of Ce- and U-based alloys would be a signature of contributions from independent impurity centers.[17] However, at larger values of concentration in a system of localized spins, the linear dependence on x does not hold, and Gor'kov and Kim[17] calculated an additional x^2 correction term to both the specific heat and magnetic susceptibility, using the Fermi liquid formulation. Therefore, the very good fit of our data to a quadratic equation relating m^* and x would indicate that impurity centers are coupled even at low Ce concentrations. This observation is consistent with the model of coupled Ce atoms giving rise to the antiquadrupolar state in CeB_6.[18] We would like to point out that the effective mass m^* could be spin-dependent. At this stage in the analysis, the effective mass m^* is the one determined from the temperature dependence

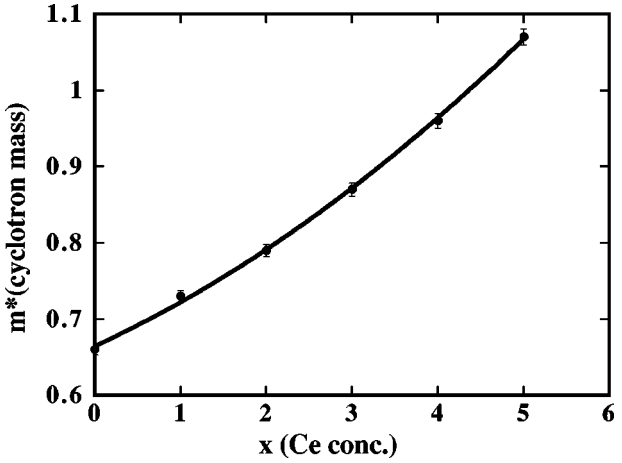

FIG. 5. The Ce concentration dependence of cyclotron mass for the α_3 orbit at 10 T. The solid line is a quadratic fit to the data.

of the overall dHvA signal without regard to the detailed contributions from spin-up and spin-down electrons. The spin dependence of m^* will be discussed later in Sec. V.

In the usual case when both spin states have the same mass, the magnetic field dependence of the dHvA amplitude can be used to determine the average Dingle temperature $\overline{T}_D$ for the two spin states (see Sec. V). The effect of finite relaxation time due to impurity or point defects is to broaden the Landau levels, leading to a reduction in amplitude roughly equivalent to that which would be caused by a rise of temperature to $\overline{T}_D$. The field dependence of the dHvA amplitude can be expressed as[16]

$$A_p = \frac{C_p T H^{-n} R_D}{\sinh(\alpha p T/H)}, \tag{2}$$

where A_p is the amplitude of the pth harmonic, $R_D = \exp(-\alpha p \overline{T}_D/H)$ is the Dingle reduction factor, p is the harmonic number, $\alpha = 14.69(m^*/m_e)$ T/K, and C_p and n depend on the particular method of measurement. For the torque method the value of $n = -1/2$ and a plot of $\ln[A_p H^{-1/2} \sinh(\alpha p T/H)]$ versus $1/H$ yields a straight line with a slope of $\alpha p \overline{T}_D$ and a linear fit to the data gives $m^* \overline{T}_D$. A Dingle plot for the high field cantilever data for 1% Ce in LaB_6 at $T = 1.73$ K and in the field range 10–25 T is given in Fig. 6. From the slope of the straight line the value of the average Dingle temperature $\overline{T}_D$ was found to be 3.5 K at high fields on the assumption that $m = 0.73 m_e$ for both spin states. We have analyzed the field dependence of the amplitude for all six samples ($0 \leqslant x \leqslant 0.05$) using field modulation in the range $7 \leqslant B \leqslant 15$ T and we find that $m^* \overline{T}_D$ obtained simply from the overall field dependence of the total signal amplitude is the same within the measurement uncertainty. This means that the arbitrary substitution of La by Ce (or Ce by La) contributes little or nothing to the mean free path l of the electrons giving rise to the signals. The mean free path is given by

$$\frac{l}{l_c} = \omega_c \tau, \tag{3}$$

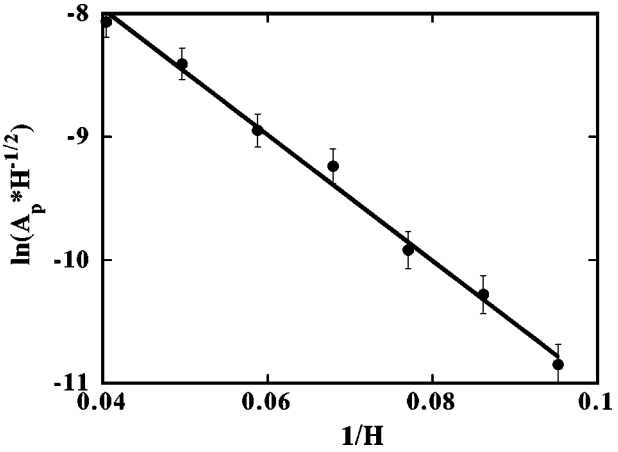

FIG. 6. Dingle plot for $x = 0.01$ at 1.73 K in the field range of 10–25 T using the cantilever technique.

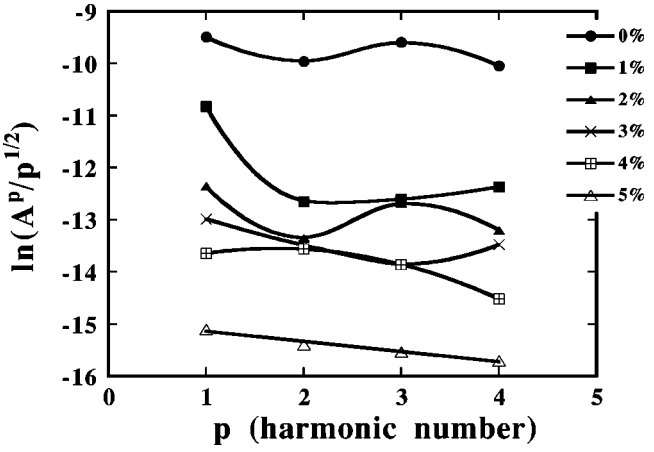

FIG. 7. A plot of $\ln(A_p/p^{1/2})$ versus the harmonic number p for $x = 0$ to 0.05. Note that it becomes linear at $x = 0.05$.

where l_c is the cyclotron length for a particular orbit given by[10]

$$l_c = \left(\frac{2\hbar F}{eB^2} \right)^{1/2}. \tag{4}$$

The average scattering rate is related to the average Dingle temperature by the relation

$$\overline{T}_D = \frac{\hbar}{2\pi k \tau}. \tag{5}$$

Thus, since $m^* \overline{T}_D$ is independent of x to within experimental uncertainty, the mean free path l is also independent of x for a given field range. This observation is in agreement with our earlier results[10] that the dominant source of scattering for the observed signals originates from other mechanisms and not from the substitution of La by Ce. However, it will be seen in the next section that if the masses are different for the two spin states, the concentration dependence of $m^{\downarrow} T_D^{\downarrow} - m^{\uparrow} T_D^{\uparrow}$ is nonzero, indicating that the contributions to the dHvA amplitude from the two spin states are unequal.

V. SPIN-DEPENDENT SCATTERING

One of the effects of an applied magnetic field is to lift the spin degeneracy of the energy levels and the contributions to the dHvA signal from the spin-up and spin-down electrons. In conventional metals, the effect of the Zeeman splitting is to reduce the amplitude by a spin reduction factor R_S given by[16]

$$R_S = \cos\left(\frac{1}{2} p \pi g \frac{m^*}{m_e} \right) \equiv \cos(p \pi S), \tag{6}$$

where g is the spin-splitting factor and m_e is the free electron mass. We had reported earlier that above 5% Ce in LaB_6, the contribution to the dHvA amplitude, originates from a single spin FS. One explanation of this observation is that scattering from spin fluctuations does not occur with equal strength for the two spin directions. There is a large negative magnetoresistance[19] in $Ce_xLa_{1-x}B_6$ alloys that can be explained by the suppression of spin fluctuation scattering. However, from magnetoresistance measurements one cannot determine if one or two spin states are contributing to the scattering. Part of the purpose of the present work was to study in detail how the single-spin dHvA signal develops in CeB_6 from the two-spin signal in pure LaB_6.

In the presence of high magnetic fields, if there is only one spin contribution to the signal, then a plot of $\ln(A_p/p^{1/2})$ against the harmonic number p yields a straight line because the spin-splitting reduction factor as is given by Eq. (6) is no longer present. However, if there are contributions to the dHvA amplitude from spin-up and spin-down states, there is spin reduction of the amplitude, and we observe a nonlinear dependence of $\ln(A_p/p^{1/2})$ on p as shown in Fig. 7 for $0 \leqslant x \leqslant 0.05$ except for $x \geqslant 0.05$, the concentration at which only one spin component is observed.

For pure LaB_6, the dHvA amplitudes associated with the spin-up and spin-down electrons are equal. However, if magnetic impurities are involved, we could expect spin-dependent scattering (SDS), and the amplitudes for spin-up and spin-down oscillations could be unequal corresponding to unequal Dingle temperatures and unequal masses. So, the signal amplitude measured with the field modulation technique, which has contributions from both the spin-up and spin-down components, has to be modified in order to account for differences in Dingle temperatures and masses between the two spin channels. In the first harmonic detection, this signal voltage is related to the oscillatory magnetization by[20]

$$\tilde{V}(\zeta) = G \sum_p \tilde{M}_p J_1(p\Lambda) \sin(p\zeta + \theta_p), \tag{7}$$

where G represents the system gain, $\tilde{M}_p$ is the magnetization due to the pth harmonic of the dHvA signal, J_1 is a Bessel function of order one, $\Lambda = 2\pi h/H^2$, h is the modulation amplitude, $\zeta = 2\pi F/H$, $\sigma = \pm 1$, and θ_p is the phase. The magnetization $\tilde{M}$ can be written as[20]

$$\tilde{M} = \sum_{p=1}^{\infty} \sum_{\sigma} C_p D^p E^{\sigma p} \sin\left(p\zeta + p\frac{\pi}{4} - \sigma p \pi S \right), \tag{8}$$

where

$$D = \exp(-Km^* \overline{T}_D / H), \tag{9}$$

$$\overline{T_D} = (T_D^{\downarrow} + T_D^{\uparrow})/2, \tag{10}$$

$$E = \exp[-Km^*(\delta T_D)/H], \tag{11}$$

$$\delta T_D = (T_D^{\downarrow} - T_D^{\uparrow})/2, \tag{12}$$

and

$$C_p = \frac{\nu TF}{(A'' p\hbar)^{1/2}} \frac{1}{\sinh(pKm^*T/H)}, \tag{13}$$

where $\nu = 1.304 \times 10^{-5}$ $\mathrm{Oe}^{1/2}/\mathrm{K}$, $K = 14.69$ (T/K), F is the dHvA frequency, and A is the extremal cross sectional area of the FS.

If the phase difference ϕ_p $(= p\pi S)$ between spin-up and spin-down oscillations is field dependent, the first two harmonics of the magnetization $\tilde{M}$ may also be written as

$$\tilde{M}_1 = C_1 \left[z \sin\left(\psi + \frac{\phi}{2} \right) + z' \sin\left(\psi - \frac{\phi}{2} \right) \right] \tag{14}$$

$$= C_1 (z^2 + z'^2 + 2zz' \cos\phi)^{1/2} \sin(\psi + \theta_1) \tag{15}$$

and

$$\tilde{M}_2 = C_2 [z^4 + z'^4 + 2z^2 z'^2 \cos(2\phi)]^{1/2} \sin\left(2\psi \mp \frac{\pi}{4} + \theta_2 \right), \tag{16}$$

where z is the Dingle reduction factor for the spin up electrons, z' is the Dingle reduction factor for the spin-down electrons, and ψ is defined to be $2\pi F/H \pm \pi/4$, where the upper sign is for a minimum FS area and the lower is for a maximum FS area. Other higher harmonics can be written in a similar way. The relative phase between the spin-up and -down components of the signal is given by

$$\tan\theta_p = \frac{z^p - z'^p}{z^p + z'^p} \tan\left(\frac{p\phi}{2} \right), \tag{17}$$

and the spin-up and the spin-down Dingle reduction factors for the pth harmonic are given by

$$z^p = \exp(-p\alpha T_D^{\uparrow}/H) \tag{18}$$

and

$$z'^p = \exp(-p\alpha T_D^{\downarrow}/H). \tag{19}$$

The relative phases are obtained by fitting the data to the first three harmonics of the magnetization. From the measured signal harmonic amplitude ratios M_2/M_1 and M_3/M_1 and the relative phases between the harmonics $\theta_2 - 2\theta_1$ and $\theta_3 - 3\theta_1$, we calculate, at a given H and T, the values of the amplitudes D and E (i.e., $m^* \overline{T_D}$ and $m^* \delta T_D$) and the value of S or ϕ_p. Once the value of S is known, we can determine the amplitude ratio $z' C_p^{\downarrow}/z C_p^{\uparrow}$ (or $m^{\downarrow} T_D^{\downarrow} - m^{\uparrow} T_D^{\uparrow}$). Since $m^* \overline{T_D}$ is the average of the contributions to the dHvA amplitudes from both spins, it is not possible from this to determine the spin dependence of T_D or m^*. However, if

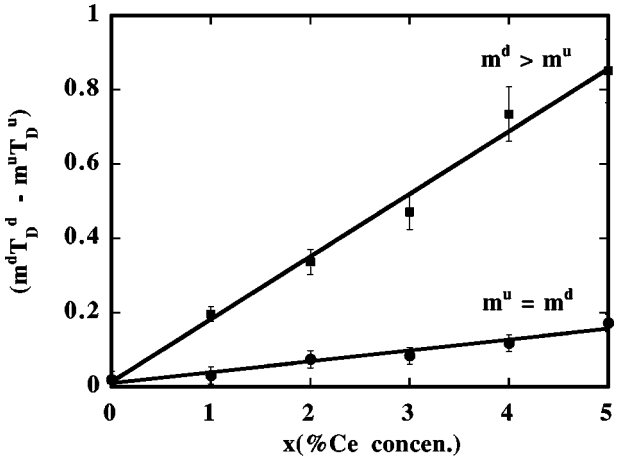

FIG. 8. Ce concentration dependence of $m^{\downarrow} T_D^{\downarrow} - m^{\uparrow} T_D^{\uparrow}$.

$m^{\downarrow} T_D^{\downarrow} - m^{\uparrow} T_D^{\uparrow}$ is nonzero, then we can determine that the product $m^* T_D$ is spin-dependent even though it is not trivial to single out the spin dependence of m^* or T_D. Therefore, if we first assume that m^* is spin-independent or $m^{\uparrow} = m^{\downarrow}$ so that C_p [Eq. (13)] is the same for both spin states, then $m^{\downarrow} T_D^{\downarrow} - m^{\uparrow} T_D^{\uparrow}$ reduces to $m^*(T_D^{\downarrow} - T_D^{\uparrow})$ and the concentration dependence of $m(T_D^{\downarrow} - T_D^{\uparrow})$ shows the dependence of the Dingle temperature. On the other hand, if m^* is spin-dependent or $m^{\uparrow} \neq m^{\downarrow}$, then $C_p^{\downarrow} \neq C_p^{\uparrow}$ and the x dependence of $m^{\downarrow} T_D^{\downarrow} - m^{\uparrow} T_D^{\uparrow}$ as compared to that of $m(T_D^{\downarrow} - T_D^{\uparrow})$ shows the spin dependence of m^* in addition to that of T_D. These two expressions are plotted against x as shown in Fig. 8. The first observation is that the slopes of these two lines are nonzero, exhibiting clear evidence of SDS. Notice that the circles represent the case for $m^{\uparrow} = m^{\downarrow}$, while the squares represent the case $m^{\uparrow} \neq m^{\downarrow}$. The slope of the line corresponding to $m^{\uparrow} \neq m^{\downarrow}$ is approximately eight times that corresponding to $m^{\uparrow} = m^{\downarrow}$, indicating that $m^{\downarrow} T_D^{\downarrow}$ becomes greater than $m^{\uparrow} T_D^{\uparrow}$ as the Ce concentration increases, that additional large increase in slope arising from the difference in mass.

For LaB_6, the two spin components have equal amplitudes and the amplitude ratio z'/z is equal to one or $\delta T_D = T_D^{\downarrow} - T_D^{\uparrow} = 0$. In other words, the scattering rates for spin up and spin down are equal. As the Ce concentration is increased to 5%, the ratio of the spin-up to the spin-down dHvA amplitude increases so that the observed dHvA signals at 5% Ce in LaB_6 arise from one spin channel, which is the spin-up channel.

There are two contrasting theories concerning whether the properties of the FS are dominated by the spin-up or spin-down states. The first is the theory developed by Wasserman *et al.*[21] for quantum oscillations in heavy-fermion materials. This model, along with its zero-field predecessor,[22] is successful in accounting for the heavy effective masses as well as small topological changes in the FS caused by the presence of additional f electrons. However, this model also predicts that the dHvA signal is dominated by the spin-down channel, and that its associated effective mass should decrease in a magnetic field. While apparent evidence for this was reported in very heavy compounds such as $CeCu_6$,[23] it is CeB_6 that shows perhaps the most dramatic mass changes

with increasing magnetic field,[24] but the polarity of the spin was not identified.

A large number of dHvA measurements have been performed on CeB_6,[25–33] which is regarded as a typical dense Kondo lattice with a very low Kondo temperature of 1–2 K. Previous experimental data have appeared to be entirely consistent with the theoretical model of Wasserman *et al.*,[21] that is, the effective mass is dramatically suppressed in a magnetic field.[24] Recent measurements[9] have shown that in addition to the suppression of the effective mass, there is notable deformation in the topology of the FS in a magnetic field, and this result is not entirely consistent with the mean-field theory of Ref. 21. One aspect of the result that does appear to be consistent with this theoretical model, though, is that the dHvA signal originates from only a single-spin FS sheet,[9] even though the theory must be fundamentally incorrect because it predicts the wrong spin state to be observed.

All of the dHvA measurements on CeB_6 are made in the high-magnetic-field regime well above the metamagnetic transition where the dipole moments of the *f* electrons are essentially aligned. According to Edwards and Green,[34] in this regime the theory developed by Wasserman *et al.*[21] is no longer applicable. This is due to the fact that this is a mean-field approach in which the interactions are assumed not to change in a magnetic field. Making such a description of the dHvA effect in HF systems is really only valid at low magnetic fields, that is, magnetic fields less than the Kondo temperature scale. Edwards and Green[34] instead make the analogy of a HF compound in a magnetic field to a itinerant ferromagnet, in which spin fluctuations play a decisive role. Edwards and Green[34] also anticipate that the dHvA effect should be dominated by only a single spin, but the up spin instead of the down spin. Therefore, one can see that our measurements are in agreement with the predictions of Edwards and Green that the down-spin mass enhancement is larger than that of the up spin and does not contribute to the dHvA signal amplitude.

As further verification of this mass difference, we use Eqs. (13), (18), and (19) to write

$$-\frac{H}{K}\ln(zC_p^{\uparrow}/z'C_p^{\downarrow})=(m^{\downarrow}-m^{\uparrow})T+(m^{\downarrow}T_D^{\downarrow}-m^{\uparrow}T_D^{\uparrow}). \tag{20}$$

In deriving Eq. (20) we replace $\sinh(y)$ with $\exp(y)$ because all values of the exponent y are much greater than 1. The quantity on the left hand side of Eq. (20) is calculated for each value of x and plotted versus T in Fig. 9. It can be seen that the data is linear in T with a slope of $m^{\downarrow}-m^{\uparrow}$ and intercept $m^{\downarrow}T_D^{\downarrow}-m^{\uparrow}T_D^{\uparrow}$. The value of $m^{\downarrow}-m^{\uparrow}$ ranges from 0.003 for $x=0$ or pure LaB_6 to 0.09 for $x=0.05$, respectively. In addition, the value of $m^{\downarrow}T_D^{\downarrow}-m^{\uparrow}T_D^{\uparrow}$ ranges from 0.03 for $x=0$ to 0.3 for $x=0.05$. Thus, for pure LaB_6, where both spin states are observed, $m^{\downarrow}=m^{\uparrow}$ as expected. As the Ce concentration increases to 5%, $m^{\downarrow}-m^{\uparrow}$ increases with $m^{\downarrow}$ being greater than $m^{\uparrow}$ by about 10%. If this mass difference continues to increase with x the observed discrepancy between specific heat and dHvA mass measurements in CeB_6 is explained. Moreover, the difference in the scattering parameter, $m^{\downarrow}T_D^{\downarrow}-m^{\uparrow}T_D^{\uparrow}$, increases with the Ce concentration, confirming that the observed FS is due only to the spin-up state.

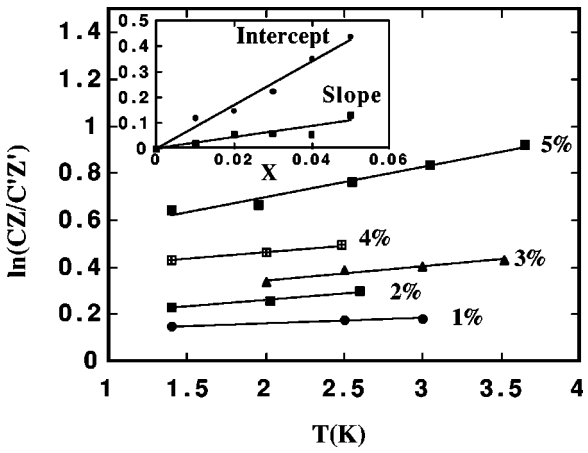

FIG. 9. Temperature dependence of $(H/K)\ln(Cz/C'z')$ for all the alloys including pure LaB_6. From the linear fits to the data, mass differences between the two spin states were determined from the slopes and intercepts. The inset shows the slopes and intercepts as a function of x.

These observations lead us to the conclusion that it is the combination of Δm^* and SDS that takes the down spin out of the dHvA signal. Therefore, both Δm^* and SDS are equally important in understanding many of the properties of CeB_6.

VI. CONCLUSION

We have performed a detailed microscopic dHvA study of low concentration (up to $x=0.05$) in $Ce_xLa_{1-x}B_6$ alloys and determined the development of the size and geometry of the FS from that of LaB_6 to the observed single spin state of $Ce_xLa_{1-x}B_6(x\geqslant 0.05)$ alloys. We have shown the following.

(1) The spin-up signal amplitude dominates the dHvA signal when the Ce concentration is $\geqslant 5\%$.

(2) We determined that the down-spin mass is greater than that of the up spin, and the spin-down contribution to the dHvA signal amplitude is small.

(3) The angular dependence of the dHvA extremal areas of the FS show that the assumption that the FS is an ellipsoid of revolution is valid for all concentrations measured.

(4) The dependence of the effective mass on concentration is in agreement with the existing theories of magnetic impurity interactions.[17]

Overall, this work presents a very detailed analysis of dHvA measurements in alloy systems involving magnetic ions with concentrations greater than 1%.

ACKNOWLEDGMENTS

A portion of this work was performed at the National High Magnetic Laboratory, which is supported by NSF Cooperative Agreement No. DMR-9527035 and by the State of Florida. Additional support from the NSF (DMR9971348) is acknowledged by one of us, Z.F.

[1] A. P. J. Arko, G. Crabtree, D. Karim, F. M. Mueller, and L. R. Windmiller, Phys. Rev. B **13**, 5240 (1976).
[2] P. Nyhus, S. L. Cooper, Z. Fisk, and J. Sarrao, Phys. Rev. B **55**, 12 488 (1997).
[3] H. C. Longuet-Higgins and M. de V. Roberts, Proc. R. Soc. London, Ser. A **224**, 336 (1954).
[4] W. A. C. Erkelens, L. P. Regnault, P. Burlet, J. Rossatmignod, S. Kunii, and T. Kasuya, J. Magn. Magn. Mater. **63/64**, 61 (1987).
[5] D. P. Young, D. Hall, M. E. Torelli, Z. Fisk, J. L. Sarrao, J. D. Thompson, H. R. Ott, S. B. Oseroff, R. G. Goodrich, and R. Zysler, Nature (London) **397**, 412 (1999).
[6] S. Sullow, I. Prasad, M. C. Aronson, J. L. Sarrao, Z. Fisk, D. Hristova, A. H. Lacerda, M. F. Hundley, A. Vigliante, and D. Gibbs, Phys. Rev. B **57**, 5860 (1998).
[7] L. Degiorgi, E. Felder, H. R. Ott, J. L. Sarrao, and Z. Fisk, Phys. Rev. Lett. **79**, 5134 (1997).
[8] A. P. J. van Deursen, Z. Fisk, and A. R. de Vroomen, Solid State Commun. **44**, 609 (1982).
[9] N. Harrison, D. W. Hall, R. G. Goodrich, J. J. Vuillemin, and Z. Fisk, Phys. Rev. Lett. **81**, 870 (1998).
[10] R. G. Goodrich, N. Harrison, A. Teklu, D. Young, and Z. Fisk, Phys. Rev. Lett. **82**, 3669 (1999).
[11] R. G. Goodrich, N. Harrison, J. J. Vuillemin, A. Teklu, D. W. Hall, Z. Fisk, D. Young, and J. Sarrao, Phys. Rev. B **58**, 14 896 (1998).
[12] M. R. Halse, Philos. Trans. R. Soc. London, Ser. A **265**, 53 (1969).
[13] Y. Onuki, T. Komatsubara, P. H. P. Reinders, and M. Springford, J. Phys. Soc. Jpn. **58**, 3698 (1989).
[14] N. Harrison, R. G. Goodrich, J. J. Vuillemin, Z. Fisk, and D. G. Rickel, Phys. Rev. Lett. **80**, 4498 (1998).
[15] Y. Ishizawa, H. Nozaki, T. Tanaka, and T. Nakajima, J. Phys. Soc. Jpn. **48**, 1439 (1980).
[16] D. Shoenberg, *Magnetic Oscillations in Metals* (Cambridge University Press, Cambridge, 1984).
[17] L. P. K. Gor'kov and Ju H. Kim, Phys. Rev. B **51**, 3970 (1995).
[18] F. J. Ohkawa, J. Phys. Soc. Jpn. **52**, 3897 (1983).
[19] N. Sato, A. Sumiyama, S. Kunii, H. Nagano, and T. Kasuya, J. Phys. Soc. Jpn. **54**, 1923 (1985).
[20] H. G. Alles, R. J. Higgins, and D. H. Lowndes, Phys. Rev. Lett. **30**, 705 (1973).
[21] A. Wasserman, M. Springford, and F. Han, J. Phys.: Condens. Matter **3**, 5335 (1991).
[22] J. W. Rasul, Phys. Rev. B **39**, 663 (1989).
[23] S. B. Chapman, M. Hunt, P. Meeson, and M. Springford, Physica B **163**, 361 (1990).
[24] N. Harrison, P. Meeson, P -A. Probst, and M. Springford, J. Phys.: Condens. Matter **5**, 7435 (1993).
[25] A. P. J. van Deursen, R. E. Pols, A. R. de Vroomen, and Z. Fisk, J. Less-Common Met. **111**, 331 (1985).
[26] W. Joss, J. M. van Ruitenbeek, G. W. Crabtree, J. L. Tholence, A. P. J. van Deursen, and Z. Fisk, Phys. Rev. Lett. **59**, 1609 (1987).
[27] T. Goto, T. Suzuki, Y. Ohe, S. Sakatsume, S. Kunii, T. Fujimura, and T. Kasuya, J. Phys. Soc. Jpn. **57**, 2885 (1988).
[28] W. Joss, J. M. van Ruitenbeek, G. W. Crabtree, J. L. Tholence, A. P. J. van Deursen, and Z. Fisk, J. Phys. (France) **49**, 747 (1988).
[29] W. Joss, J. Magn. Magn. Mater. **84**, 264 (1990).
[30] Y. Onuki, T. Komatsubara, P. H. P. Reinders, and M. Springford, Physica B **163**, 100 (1990).
[31] E. G. Haanappel, R. Hedderich, W. Joss, S. Askenazy, and Z. Fisk, Physica B **177**, 181 (1992).
[32] H. Matsui, T. Goto, S. Kunii, and S. Sakatsume, Physica B **186-188**, 126 (1993).
[33] R. W. Hill, C. Haworth, T. J. B. M. Janssen, P. J. Meeson, M. Springford, and A. L. Wassermann, Physica B **230-232**, 114 (1997).
[34] D. M. Edwards and A. C. Green, Z. Phys. B: Condens. Matter **103**, 243 (1997).